UNCLASSIFIED

Defense Technical Information Center
Compilation Part Notice

ADP010713

TITLE: Test Cases for Flutter of the Benchmark Models Rectangular Wings on the Pitch and Plunge Apparatus

DISTRIBUTION: Approved for public release, distribution unlimited

This paper is part of the following report:

TITLE: Verification and Validation Data for Computational Unsteady Aerodynamics [Donnees de verification et de valadation pour l'aerodynamique instationnaire numerique]

To order the complete compilation report, use: ADA390566

The component part is provided here to allow users access to individually authored sections of proceedings, annals, symposia, ect. However, the component should be considered within the context of the overall compilation report and not as a stand-alone technical report.

The following component part numbers comprise the compilation report:

ADP010704 thru ADP010735

UNCLASSIFIED

7E. TEST CASES FOR FLUTTER OF THE BENCHMARK MODELS RECTANGULAR WINGS ON THE PITCH AND PLUNGE APPARATUS

Submitted by

Robert M. Bennett
Senior Aerospace Engineer
Aeroelasticity Branch, Structures and Materials
Mail Stop 340
NASA Langley Research Center
Hampton, VA 23681-2199 USA
r.m.bennett@larc.nasa.gov

INTRODUCTION

As a portion of the Benchmark Models Program at NASA Langley (Ref 1), three models with the same rectangular planform, but with different airfoils were flutter tested on the Pitch and Plunge Apparatus (PAPA, Ref 2-3). These models were designed and tested to provide flutter data for evaluating Computational Aeroelasticity (CA) programs with emphasis on transonic flows. The geometry of the wings was kept simple to reduce the complexity of the geometry processing for computation and in the interpretation of the results. One model was built with the NACA 0012 airfoil called the B0012, one with the NACA 64A010 airfoil called the B64A010, and one with an NASA SC(2)-0414 airfoil called BSCW. These airfoils, shown in Fig 1, were not selected to provide a systematic empirical trend study of thickness or airfoil type, but to provide flutter data for wings with different transonic airfoil characteristics. The NACA 0012 airfoil has a forward loading and for transonic flows, a shock forms initially ahead of midchord. The NACA 64A010 airfoil has a more mild evolution of the shock which forms initially near midchord. The NASA SC(2)-0414 has a strong aft loading and the associated low aft upper surface curvature. There was considerable experience in two dimensions with the NACA 0012 and 64A010 airfoils based on comparisons with the early two-dimensional unsteady aerodynamic data of Ref 4. The supercritical airfoil (Ref 5) was chosen as a relatively modern airfoil for comparison.

The B0012 model was tested first. Three different types of flutter instability boundaries were encountered, a classical flutter boundary, a transonic stall flutter boundary at angle of attack, and a plunge instability near M = 0.9 and for zero angle of attack. This test was made in air and was Transonic Dynamics Tunnel (TDT) Test 468 (Ref 1, 6-8). The BSCW model (for Benchmark SuperCritical Wing) was tested next as TDT Test 470 (Ref 9-11). It was tested using both with air and a heavy gas, R-12, as a test medium. The effect of a transition strip on flutter was evaluated in air. The B64A010 model was subsequently tested as TDT Test 493 (Ref 1).

Some further analysis of the experimental data for the B0012 wing is presented in Ref 12. Transonic calculations using the parameters for the B0012 wing in a two-dimensional typical section flutter analysis are given in Ref 13.

These data are supplemented with data from the Benchmark Active Controls Technology model (BACT) given in Ref 14-15 and in the next chapter of this document. The BACT model was of the same planform and airfoil as the B0012 model, but with spoilers and a trailing edge control. It was tested in the heavy gas R-12, and was instrumented mostly at the 60 per cent span. The flutter data obtained on PAPA and the static aerodynamic test cases from BACT serve as additional data for the B0012 model. All three types of flutter are included in the BACT Test Cases.

In this report several test cases are selected to illustrate trends for a variety of different conditions with emphasis on transonic flutter. Cases are selected for classical and stall flutter for the BSCW model, for classical and plunge for the B64A010 model, and for classical flutter for the B0012 model. Test Cases are also presented for BSCW for static angles of attack. Only the mean pressures and the real and imaginary parts of the first harmonic of the pressures are included in the data for the test cases, but digitized time histories have been archived. The data for the test cases are available as separate electronic files. An overview of the model and tests is given, the standard formulary for these data is listed, and some sample results are presented.

LIST OF SYMBOLS AND DEFINITIONS

a	speed of sound,ft/sec
A_z	amplitude of the plunge free vibration envelope, inches
A_θ	amplitude of the pitch free vibration envelope, degrees
b	semichord, c/2
c	wing chord, ft (m)
C_p	pressure coefficient, $(p - p_\infty) / q_\infty$ steady; $(p - p_{mean}) / q_\infty$ unsteady
f	frequency, Hz
h	plunge displacement, inches

k	reduced frequency, $\omega c/(2V_\infty)$
M	Mach number
p	pressure, psf
p_∞	freestream static pressure, psf
q_∞	dynamic pressure, psf (kPa)
s	semispan, 32 inches
R_n	Reynolds number based on chord
T_o	total or stagnation temperature, °R
V_∞	freestream velocity, ft/sec (m/sec)
V	velocity, ft/sec (m/sec)
V_I	flutter speed index, $V_f / \left(b\omega_\theta\sqrt{\mu}\right)$
x/c	streamwise fraction of local chord
y	spanwise coordinate normal to freestream
α_m	mean angle of attack, degrees
ϕ	phase angle referenced to pitch displacement, degrees
θ	pitch angle, degrees
η	fraction of span, y/s
μ	mass ratio, wing mass/$\left(\pi b^2 \rho \text{span}\right)$
ρ	density
γ	ratio of specific heats for test gas
ω	frequency, radians/second
ζ_z	fraction of critical damping for plunge
ζ_θ	fraction of critical damping for pitch
$\lvert\ \rvert$	absolute value

subscripts

0	steady value
f	flutter
m	mean value
h	plunge mode
z	vertical displacement
θ	pitch mode

MODEL AND TESTS

The BMP rectangular wing models were tested in the NASA Langley Transonic Dynamics Tunnel (TDT). The tunnel has a slotted test section 16-feet (4.064 m) square with cropped corners. At the time of these tests, it could be operated with air or a heavy gas, R-12, as a test medium at pressures from very low to near atmospheric values. Currently the TDT can be operated with air or R-134a as a test medium. An early description of this facility is given in Ref 16 and more recent descriptions of the facility are given in Ref 17 and 18. The early data system is described in Ref 19 and the recent data system given in Ref 20 and 21, but the data system used in the BMP tests was a version between these systems. Based on cone transition results (Ref 22-23), the turbulence level for this tunnel is in the average large transonic tunnel category. Some low speed measurements in air have also been presented in Ref 24.

The three wing models were very similar but differed somewhat in detail. These models were of rectangular planform with a span of 32 inches (813 mm) plus a tip of revolution, and a chord of 16 inches (406 mm). The wings were machined from aluminum, were very smooth, and were tested either with free transition or with a transition strip at 7.5 per cent chord on both upper and lower surfaces. They were fabricated in three parts as shown in Fig 2, with two main sections and a tip section to facilitate access to the pressure instrumentation.

The assembled BSCW model is shown installed in the wind tunnel in Fig 3 and an overall view of the BSCW model and splitter plate installed in the TDT test section is shown in Fig 4. The model was mounted on a large splitter plate set out approximately 40 inches (1.02 m) from tunnel sidewall. An end plate that moved with the model was attached to the root of the model, and moved within a recessed or undercut section of the splitter plate. A large fairing behind the splitter plate isolated the equipment

between the splitter plate and the tunnel sidewall from the airstream. Some recent tests (Ref 25) of the splitter plate arrangement without a wing have shown some nonuniformity of the flow along the splitter plate resulting from the flow around the leading edge of the splitter plate for Mach numbers above M = 0.80. The data for the models may be affected somewhat above M = 0.80.

These models were flutter tested using the Pitch and Plunge Apparatus (PAPA, Ref 2-3) as shown in the photograph of Fig 5 and illustrated in the sketch of Fig 6. The PAPA system permits rigid body pitch and plunge motion of the wing and flutter of the system by using four circular rods for flexibility. This system has sufficient strength to permit flutter testing at moderate angles of attack including some stall flutter cases. The rods are arranged such that the elastic axis is at the midchord and the model is balanced to place the center of gravity on the midchord. The system thus gives essentially uncoupled pitch and plunge modes about the midchord of the model. The summary of the modal parameters is given in Table 1. The generalized masses given here are the effective mass and pitch inertia calculated from the frequency and stiffness values. Higher modes of this system have been determined for the BSCW model (Ref 10) and are considered typical for all three models. Some amplitude effects on frequency and damping were analyzed (Ref 10) and can be summarized by the following equations.

$$f_z = 3.339978 - 0.638404\ A_z + 0.09185239\ A_z^2 \qquad \zeta_z = 0.0006913 + 0.0021713\ A_z$$

$$f_\theta = 5.1987 \quad - 0.008994\ A_\theta + 0.0056696\ A_\theta^2 \qquad \zeta_\theta = 0.0004379 + 0.0003561\ A_\theta$$

where A_z is the amplitude of the plunge free vibration envelope in inches, and A_θ is the amplitude of pitch free vibration envelope in degrees. The effects of amplitude are quite small for the frequencies (third or fourth significant figure) but are significant on damping. Detailed wind-off free decay records have been archived.

In addition to the testing on the PAPA, the B0012 and BSCW models were tested with the PAPA mount system rigidized for static pressure measurements. The model could be pitched statically with the turntable, but there was no balance in this system for force measurements. Only static data for BSCW are included as test cases. Static data, including force measurements, for a similar 0012 model is available in the next chapter of this document for the BACT model.

Both the model and the plate that constrains the model end of the PAPA system are large in mass. The resulting mass ratio at flutter is thus very large and consequently the reduced frequency at flutter is very low. The reduced frequency may be more comparable to those for rigid body modes for an aircraft than typical of flutter. The flutter crossings are relatively mild and unpublished calculations for the B0012 model have indicated some sensitivity to torsional aerodynamic damping.

The models were instrumented for unsteady pressures at two chords and for dynamic motions. The list of transducers is given in Table 2. The primary dynamic motion measurements were made with the PAPA strain gages and accelerometers, although four wing accelerometers were included. There were 40 unsteady pressure transducers located along the chord at 60 per cent span and 40 located at 95 per cent span. The distribution for BSCW is illustrated in figure 7. The chordwise distribution of unsteady pressure transducers was slightly different for each model and is summarized in Table 3. In addition to the pressure measurements on the wing, there were transducers located in the splitter plate as illustrated in figure 8 and listed in Table 4. However the data measured on the splitter plate are not included in the data sets for the Test Cases of these wings.

It might be noted that some flow visualization work on these low aspect ratio planforms indicated that wing surface separation tended to occur in an inboard aft cell. The row of pressure transducers at 60 per cent chord was in the outer portion of this cell, whereas the row at 95 per cent span was dominated by the tip flow.

Data from all channels were acquired simultaneously at a rate of 1000 or 500 samples/second (depending on the test) for 20 seconds for the dynamic data and for 10 seconds for the static data.. Each recorded data set was stored in digital form on disk, and assigned an index called a Point No. which is given in the Tables. Although it was intended to use 200 Hz or 400 Hz low pass filters in the data stream prior to digitizing the data to avoid aliasing, the filters were later thought to be set at 1000 Hz as a result of a data system problem. The data are thus considered aliased with a foldover frequency of 500 Hz. For the flutter data, which was in the 4 to 10 Hz range, in order for the 1st harmonic to be contaminated, there would have to be significant signals at 990-996 Hz for the 1000 samples/sec case and at 490-510 and 990-996 Hz for the 500 samples/sec cases. It is not considered likely that there are significant disturbances in these frequency ranges.

Detailed geometry measurements were performed for each of these wings along several sections. The measured ordinates are not included in this report, but they are available as electronic files. Design ordinates are given in Table 5 only for the BSCW and B64A010 models since the NACA 0012 airfoil is analytically defined. The thickness of the aft end of the NACA 64A010 airfoil was increased to permit smooth installation of the aft-facing transducers in the trailing edge. The trailing edge thickness was increased and a line was drawn to be tangent to the original airfoil. Therefore the modified B64A010 airfoil has a somewhat larger linear aft section than the standard 64A010 which is linear in thickness from 0.80 to the trailing edge. Table 5b lists the design ordinates with interpolation of the airfoil to 104 points along the chord.

TEST CASES

The flutter Test Cases for the three models on the PAPA system are listed in Tables 6-8. In the Test Case Number, the leading portion is 7E for the Chapter number, followed by the Model designation, SW = BSCW model, 64 for the B64A010 model, and 12 for the B0012 model. Flutter is denoted by F with a following letter for the type of flutter, C = classical, S = stall, and P = plunge.

The BSCW model was tested both in air and in the heavy gas, R-12. The classical flutter boundaries for both the air and R-12 tests are given in Fig 9 in terms of dynamic pressure versus Mach number and flutter frequency versus Mach number. The

flutter dynamic pressure increases with Mach number. This is an unusual trend that is apparently a result of the specific aeroelastic configuration of this model on the PAPA system. The boundary flattens near M = 0.78-0.80 and then rises which is interpreted as the transonic "dip" for this system. The boundaries obtained in air and in R-12 show generally good agreement.

A few points of stall flutter near $\alpha = 5^{o}$ and M = 0.80 were obtained with the BSCW model and are included in Table 6. The corresponding flutter boundary is given in Fig 10. The boundary is not fully defined with angle of attack, but the stall flutter boundary appears to be nearly vertical near $\alpha = 5^{o}$. These points are thought to involve shock waves and separating and reattaching flows during the cycle of motion. No plunge instability points were defined for the BSCW model, possibly because the condition of zero lift could not be obtained without hitting the stops within the mechanical setup. For the NASA supercritical airfoils of this type, the two-dimensional design lift coefficient occurs at $\alpha = 0^{o}$. For the SC(2)-0414 airfoil, the design lift coefficient is 0.4.

An earlier unpublished test of a supercritical wing on the PAPA system had indicated an effect of transition strip on flutter. It was found that a forward transition strip on the lower surface had a significant influence at the lower subsonic Mach numbers. Some variations of the transition strips were thus explored in this test with air as the test medium. A few Test Cases are included for the free transition test for BSCW in Table 6.

The Test Cases for static angles of attack for BSCW are presented in Table 9. The angles of attack given generally encompass the range of the flutter data in the Test Cases. A listing of a sample of the static data file illustrating the format is given in Fig 11. For each pressure transducer, the time-averaged mean, the minimum and maximum values, and the standard deviation (generally called channel statistics) of the pressure coefficient is listed. The static pressures for Test Cases 7ESWA24 and 7ESWA30 are presented in Fig 12. Test Case 7ESWA24 shows little lift at the instrumented chords except over the aft section, whereas for Test Case 7ESWA30 there is significant lift and a strong shock on the inboard section.

A listing of a sample of the flutter data file illustrating the format is given in Fig 13. The mean, minimum, maximum, and standard deviation are listed with the real and imaginary parts of the first harmonic of the unsteady pressures. The unsteady pressures are referenced to pitch displacement. The minimum, maximum, and standard deviation include the unsteady components and thus their interpretation is not straightforward. The mean pressures and the in-phase (or real) and the out-of-phase (or imaginary) components of the unsteady pressures for a classical flutter case, Test Case 7ESWFC6, are given in Fig 14. Similar data for a stall flutter Test Case, 7ESWA30 are presented in Fig 15. For the classical flutter case (Fig 14), the imaginary components of the pressure are small, but for the stall flutter Test Case the imaginary components of the pressure can be as large as the real components (Fig 15).

The unsteady pressures presented and included in the files have not been normalized by amplitude of motion. Case to case comparisons of pressures may need to be normalized by pitch or plunge amplitude values listed with the Test Case.

The flutter data for the B0012 model is given in Table 8. Only flutter Test Cases in air were obtained for this model and only classical flutter points are included as Test Cases. Corresponding flutter points for a model in R-12 with the NACA 0012 airfoil including stall and plunge flutter cases are given in the next Chapter for the Benchmark Active Controls Technology (BACT) model. The flutter boundaries for the B0012 and BSCW models are quite similar indicating that the supercritical design permits about two percent more thickness for corresponding transonic effects on flutter.

The flutter data for the B64A010 model is given in Table 9. It might be noted that the available flutter data for this model listed the plunge displacement to one significant figure (Table 9). For this thinner airfoil, the rise in the flutter boundary occurs at somewhat higher Mach number. No stall flutter points were defined for this model as sufficient angle of attack could not be obtained without hitting the stops within the mechanical setup. Two flutter points are included and labeled plunge flutter near M=0.95. They are of significantly lower frequency, but also include a significant pitch amplitude (Table 9).

Only the mean pressures and the real and imaginary parts of the first harmonic of the pressures are included in the data for the Test Cases, but digitized time histories have been archived. The data for the Test Cases are available as separate electronic files. For the flutter cases, calculations for flutter can be made and compared with measured boundaries. However in calculations, the analytical model can be forced to duplicate the measured combined pitch and plunge motion and the pressures compared directly. It might be noted that the transition strip (at 7.5 per cent chord) has an influence on the first transducer downstream of the strip that varies with angle of attack or other test conditions.

The files on the CD-ROM are ascii files and readme files are included. For BSCW, the file for the static data is named bscwstat and a Fortran program to read it, bscwstrd.f, is furnished. The BSCW flutter data is in file bscwflut, and the Fortran program to read it, bscwftrd.f, is included. The data files consist of contiguous data points in the sequence given in the tables. The design ordinates are on file bscwordt, and the measured ordinates are given on file bscworde. In the measured ordinates for BSCW, some points may need to be omitted as they were on the edge of the orifices. For the B0012 model, the flutter data is in file b12flut, and the Fortran program to read it, b12ftrd.f, is included. The design ordinates are on file b12ordt, and the measured ordinates are given on file b12orde. For the B64A010 model, the flutter data is in file b64flut, and the Fortran program to read it, b64ftrd.f, is included. The design ordinates are in file b64ordt, and the measured ordinates are given in file b64orde.

Note that the tests for these BMP models were conducted both in air and in the heavy gas, R-12. For CFD calculations, care must be exercised to select the correct gas properties are used for each Test Case. For R-12, the ratio of specific heats, γ, is calculated to be 1.132 to 1.135 for the conditions of the tests assuming 0.99 for the fraction of heavy gas in the heavy gas-air mixture. A value of 1.132 is suggested for use in computational comparisons. The corresponding value of Prandtl number is calculated to range from 0.77 to 0.78 for the conditions of these tests. For some cases, the calculated values of γ and Prandl number are included in the data files.

FORMULARY

1 General Description of Model

1.1	Designation	Three models, Benchmark Supercritical Wing Model, BSCW, Benchmark 0012 Model, B0012, and Benchmark 64A010 Model, B64A010
1.2	Type	Semispan wing
1.3	Derivation	Same planform as Benchmark Active Controls Model with 0012 airfoil, BACT (see Introduction)
1.4	Additional remarks	Overall view given in Fig 2 and shown mounted in tunnel in Figs 3 and 4
1.5	References	Refs 1, 6-11 describe tests and data

2 Model Geometry

2.1	Planform	Rectangular
2.2	Aspect ratio	2.0 for the panel (neglecting tip of rotation)
2.3	Leading edge sweep	Unswept
2.4	Trailing edge sweep	Unswept
2.5	Taper ratio	1.0
2.6	Twist	None
2.7	Wing centreline chord	16 inches (406.4 mm)
2.8	Semi-span of model	32 inches (812.8 mm) plus tip of rotation
2.9	Area of planform	512 sq. in. (0.3303 sq. m) neglecting tip
2.10	Location of reference sections and definition of profiles	Measured ordinates are given in files on the CDROM
2.11	Lofting procedure between reference sections	Constant design airfoil section
2.12	Form of wing-body junction	No fairing and plate overlapped at splitter plate
2.13	Form of wing tip	Tip of rotation
2.14	Control surface details	No control surfaces
2.15	Additional remarks	See Fig 1 for overview
2.16	References	Refs 1, 6-11

3 Wind Tunnel

3.1	Designation	NASA LaRC Transonic Dynamics Tunnel (TDT)
3.2	Type of tunnel	Continuous flow, single return
3.3	Test section dimensions	16 ft x 16 ft (4.064 x 4.064 m)
3.4	Type of roof and floor	Three slots each
3.5	Type of side walls	Two sidewall slots
3.6	Ventilation geometry	Constant width slots in test region
3.7	Thickness of side wall boundary layer	Model tested on large splitter plate set out approximately 40 inches (1.02 m) from tunnel side wall (see Fig 3). Some documentation of tunnel wall boundary layer in Ref 16
3.8	Thickness of boundary layers at roof and floor	Not documented
3.9	Method of measuring velocity	Calculated from static pressures measured in plenum and total pressure measured upstream of entrance nozzle of test section
3.10	Flow angularity	Not documented, considered small
3.11	Uniformity of velocity over test section	Not documented, considered nearly uniform, some nonuniformity over splitter plate above M = 0.80

3.12	Sources and levels of noise or turbulence in empty tunnel	Generally unknown. Some low speed measurements are presented in Ref 24. Cone transition measurements are presented in Ref 22 and 23
3.13	Tunnel resonances	Unknown
3.14	Additional remarks	Some tests performed in air and some in heavy gas, R-12. For R-12, ratio of specific heats, γ, is 1.132-1.135. For R-12 computations, 1.132 is recommended. For the conditions of this test, the R-12 Prandtl number is calculated to be 0.77-0.78
3.15	References on tunnel	Ref 16-18

4 Model Motion

4.1	General description	Flutter with combined pitch and plunge motions
4.2	Reference coordinate and definition of motion	Pitch and plunge motions referenced to midchord
4.3	Range of amplitude	Varies for each case, tabulated
4.4	Range of frequency	Generally 0 to 5 Hz
4.5	Method of applying motion	Self-excited flutter, measured values of pitch and plunge are listed with each data point
4.6	Timewise purity of motion	Not documented
4.7	Natural frequencies and normal modes of model and support system	See Table 1 for plunge and pitch on PAPA. For higher modes see Ref 10. Not documented for rigid strut
4.8	Actual mode of applied motion including any elastic deformation	Combined pitch and plunge measured. Very stiff model with flutter below 5 Hz with next vertical mode at 37 Hz
4.9	Additional remarks	None

5 Test Conditions

5.1	Model planform area/tunnel area	.015
5.2	Model span/tunnel height	.17
5.3	Blockage	Model less than 0.2% but splitter plate and equipment fairing is near 4%
5.4	Position of model in tunnel	Mounted from large splitter plate out from wall and on the tunnel centerline, Fig 3
5.5	Range of Mach number	0.30 to 0.90
5.6	Range of tunnel total pressure	Approximately 500 to 1000 psf (24 to 48 kPa)
5.7	Range of tunnel total temperature	512 to 576 degrees Rankine (23 to 47° C)
5.8	Range of model steady or mean incidence	-3° to 5° pitch
5.9	Definition of model incidence	From chord line of symmetric airfoils or reference chord line of BSCW
5.10	Position of transition, if free	Transition strip used
5.11	Position and type of trip, if transition fixed	Grit strip at 7.5% chord on upper and lower surfaces when used
5.12	Flow instabilities during tests	None defined
5.13	Changes to mean shape of model due to steady aerodynamic load	Not measured but considered very stiff
5.14	Additional remarks	Tests performed both in air and in heavy gas, R-12. For R-12 ratio of specific heats, γ, is 1.132-1.135. For R-12 computations, 1.132 is recommended. For the conditions of this test, the R-12 Prandtl number is calculated to be 0.77-0.78. Some data files include values of γ and Prandl number
5.15	References describing tests	Refs 1, 6-11

6 Measurements and Observations

6.1	Steady pressures for the mean conditions	BSCW only
6.2	Steady pressures for small changes from the mean conditions	no
6.3	Quasi-steady pressures	no
6.4	Unsteady pressures	yes
6.5	Steady section forces for the mean conditions by integration of pressures	no
6.6	Steady section forces for small changes from the mean conditions by integration	no
6.7	Quasi-steady section forces by integration	no
6.8	Unsteady section forces by integration	no
6.9	Measurement of actual motion at points of model	yes
6.10	Observation or measurement of boundary layer properties	no
6.11	Visualisation of surface flow	no
6.12	Visualisation of shock wave movements	no
6.13	Additional remarks	no

7 Instrumentation

7.1	Steady pressure	
7.1.1	Position of orifices spanwise and chordwise	40 locations at 60% span and 40 at 95% span. See Fig 7 and Table 3
7.1.2	Type of measuring system	Used same transducers as unsteady pressure measurements
7.2	Unsteady pressure	
7.2.1	Position of orifices spanwise and chordwise	Same transducers as steady measurements. See Fig 7 and Table 3
7.2.2	Diameter of orifices	.020 inches (.51 mm)
7.2.3	Type of measuring system	In situ pressure gages
7.2.4	Type of transducers	Kulites
7.2.5	Principle and accuracy of calibration	Statically calibrated and monitored through reference tubes
7.3	Model motion	
7.3.1	Method of measuring motion reference coordinate	Strain gages on PAPA system
7.3.2	Method of determining spatial mode of motion	Wind-off verification with accelerometers
7.3.3	Accuracy of measured motion	Undocumented
7.4	Processing of unsteady measurements	
7.4.1	Method of acquiring and processing measurements	Analog signals digitized at 500 or 1000 samples/sec for 10-20 seconds depending on data type
7.4.2	Type of analysis	Fourier analysis
7.4.3	Unsteady pressure quantities obtained and accuracies achieved	Amplitude and phase of each pressure signal. Accuracy not specified
7.4.4	Method of integration to obtain forces	None
7.5	Additional remarks	None
7.6	References on techniques	Data system for test similar to one described in Refs 19-20

8 Data Presentation

8.1	Test Cases for which data could be made available	See Ref 6-11
8.2	Test Cases for which data are included in this document	See Tables 6-9
8.3	Steady pressures	BSCW only
8.4	Quasi-steady or steady perturbation pressures	BSCW only given in CDROM
8.5	Unsteady pressures	C_p real and imaginary parts for first harmonic only included in CDROM. Time histories have been archived. Pressures have not been normalized by motion amplitude
8.6	Steady forces or moments	None
8.7	Quasi-steady or unsteady perturbation forces	None
8.8	Unsteady forces and moments	None
8.9	Other forms in which data could be made available	Time histories archived
8.10	Reference giving other representations of data	Ref 12

9 Comments on Data

9.1	Accuracy	
	9.1.1 Mach number	Not documented
	9.1.2 Steady incidence	Unknown
	9.1.3 Reduced frequency	Should be accurate
	9.1.4 Steady pressure coefficients	Not documented
	9.1.5 Steady pressure derivatives	None
	9.1.6 Unsteady pressure coefficients	Each gage individually calibrated and monitored statically through reference tubes
9.2	Sensitivity to small changes of parameter	None indicated. Amplitudes of oscillation varied in tests
9.3	Non-linearities	Many flow conditions involve shock waves and separation
9.4	Influence of tunnel total pressure	Not evaluated. Most of the tests at nearly constant dynamic pressure
9.5	Effects on data of uncertainty, or variation, in mode of model motion	Unknown, not expected to be appreciable
9.6	Wall interference corrections	None applied
9.7	Other relevant tests on same model	None
9.8	Relevant tests on other models of nominally the same shapes	Aerodynamic and flutter tests on similar 0012 model with spoilers and trailing edge control surface (BACT), Ref 15 and next Chapter
9.9	Any remarks relevant to comparison between experiment and theory	Some included under Model and Tests
9.10	Additional remarks	None
9.11	References on discussion of data	Ref 1 and 6-13

10 Personal Contact for Further Information

Head, Aeroelasticity Branch
Mail Stop 340
NASA Langley Research Center
Hampton, VA 23681-2199 USA

Phone: +1-(757)-864-2820
FAX: +1-(757)-864-8678

LIST OF REFERENCES

1 Bennett, Robert M.; Eckstrom, Clinton V.; Rivera, Jose, A.; Dansberry, Bryan E.; Farmer, Moses G.; and Durham, Michael H.: *The Benchmark Aeroelastic Models Program - Description and Highlights of Initial Results.* Paper No. 25 in Transonic Unsteady Aerodynamics and Aeroelasticity, AGARD CP 507, Mar. 1992. Also available as NASA TM-104180, 1991.

2 Farmer, Moses G.: *A Two-Degree-of-Freedom Flutter Mount System with Low Damping for Testing Rigid Wings at Different Angles of Attack.* NASA TM 83302, 1982.

3 Farmer, Moses G.: Mount System for Testing Flutter. U.S Patent No. 4,475,385, Oct. 9, 1984.

4 *"Compendium of Unsteady Aerodynamic Measurements,"* AGARD Report No. 702, Aug. 1982.

5 Harris, Charles D.: *NASA Supercritical Airfoils--A Matrix of Family-Related Airfoils*, NASA TP 2969, March 1990.

6 Rivera, Jose A., Jr.; Dansberry, Bryan E.; Durham, Michael, H.; Bennett, Robert M.; and Silva, Walter A.: *Pressure Measurements on a Rectangular Wing with A NACA 0012 Airfoil During Conventional Flutter.* NASA TM 104211, July 1992.

7 Rivera, Jose A.; Dansberry, Bryan E.; Bennett, Robert M.; Durham, Michael, H.; and Silva, Walter A.: *NACA 0012 Benchmark Model Experimental Flutter Results With Unsteady Pressure Distributions.* AIAA Paper 92-2396, Apr. 1992. Also available as NASA TM 107581, Mar. 1992.

8 Rivera, Jose A.; Dansberry, Bryan E.; Farmer, Moses G.; Eckstrom, Clinton, V.; Seidel, David A.; and Bennett, Robert M.: *Experimental Flutter Boundaries with Unsteady Pressure Distributions for the NACA 0012 Benchmark Model.* AIAA 91-1010, 1991. Also available as NASA TM 104072, 1991.

9 Dansberry, Bryan E.; Durham, Michael, H.; Bennett, Robert M.; Rivera, Jose A.; Silva, Walter A.; and Wieseman, Carol D.: *Experimental Unsteady Pressures at Flutter on the Supercritical Wing Benchmark Model.* AIAA 93-1592, Apr. 1993.

10 Dansberry, Bryan E.; Durham, Michael, H.; Bennett, Robert M.; Turnock, David L.; Silva, Walter A.; and Rivera, Jose A., Jr.: *Physical Properties of the Benchmark Models Program Supercritical Wing.* NASA TM 4457, Sep. 1993.

11 Dansberry, Bryan E.: *Dynamic Characteristics of a Benchmark Models Program Supercritical Wing.* AIAA 92-2368, Apr. 1992.

12 Finaish, F.: Frigerio, J.; and Bennett, R. M.: *Unsteady Pressure Distributions Around an Aeroelastic Wing in Transonic Flows.* AIAA Paper 95-0311, Jan. 1995.

13 Bendiksen, Oddvar O.; Hwang, Guang-Yaw; and Piersol, John: *Nonlinear Aeroelastic and Aeroservoelastic Calculations for Transonic Wings.* AIAA Paper 98-1898, April 1998.

14 Durham, Michael H.; Keller, Donald F.; Bennett, Robert M.; and Wieseman, Carol D.: *A Status Report on a Model for Benchmark Active Controls Testing.* AIAA Paper 91-1011, Apr. 1991. Also available as NASA TM 107582, 1991.

15 Scott, Robert C.; Hoadley, Sherwood T.; Wieseman, Carol D.; and Durham, Michael H.: *The Benchmark Active Controls Technology Model Aerodynamic Data.* AIAA Paper 97-0829, Jan. 1997.

16 Aeroelasticity Branch Staff: *The Langley Transonic Dynamics Tunnel.* LWP-799, Sep. 1969.

17 Cole, Stanley, R.; and Rivera, Jose, A, Jr.: *The New Heavy Gas Testing Capability in the NASA Langley Transonic Dynamics Tunnel.* Paper No. 4, presented at the Royal Aeronautical Society Wind Tunnels and Wind Tunnel Test Techniques Forum, Churchill College, Cambridge, UK, Apr. 1997.

18 Corliss, James M.; and Cole, Stanley R.: *Heavy Gas Conversion of the NASA Langley Transonic Dynamics Tunnel.* AIAA Paper 98-2710, June 1998.

19 Cole, Patricia H.: *Wind Tunnel Real-Time Data Acquisition System.* NASA TM 80081, 1979.

20 Bryant, C.; and Hoadley, S. T.: *Open Architecture Dynamic Data System at Langley's Transonic Dynamics Tunnel.* AAIA Paper 98-0343, Jan. 1998.

21 Wieseman, Carol D.; and Hoadley, Sherwood, T.: *Versatile Software Package for Near Real-Time Analysis of Experimental Data.* AIAA Paper 98-2722, June 1999.

22 Dougherty, N. Sam, Jr.: *Influence of Wind Tunnel Noise on the Location of Boundary-Layer Transition on a Slender Cone at Mach Numbers from 0.2 to 5.5. Volume I. - Experimental Methods and Summary of Results. Volume II. - Tabulated and Plotted Data.* AEDC--TR-78-44, March 1980.

23 Dougherty, N. Sam, Jr.; and Fisher, D. F.: *Boundary-Layer Transition on a 10-Deg. Cone: Wind Tunnel/Flight Correlation.* AIAA Paper 80-0154, Jan. 1980.

24 Sleeper, Robert K.; Keller, Donald F.; Perry, Boyd, III; and Sandford, Maynard C.: *Characteristics of Vertical and Lateral Tunnel Turbulence Measured in Air in the Langley Transonic Dynamics Tunnel.* NASA TM 107734, March 1993.

25 Schuster, David M: *Aerodynamic Measurements on a Large Splitter Plate for the NASA Langley Transonic Dynamics Tunnel.* Proposed NASA TM 1999.

Table 1. Measured Nominal Structural Dynamic Parameters

	Plunge Mode	Pitch Mode
Frequency	3.33 Hz.	5.20 Hz.
Stiffness	2637 lb/ft	2964 ft-lb/rad
Damping Ratio, ζ	0.001	0.001
Effective Mass or Inertia	6.01 slugs	2.78 slug-ft^2

Table 2. Instrumentation

Instrument	Quantity
Model Pressure Transducers	80
Splitter Plate Pressure Transducers	20
Boundary Layer Rake Pressure Transducers	10
Model Accelerometers	4
PAPA Strain Gage Bridges	2
PAPA Accelerometers	2
Turntable AOA Accelerometer	1
Model AOA Accelerometer	1

Table 3. Nominal Location of Wing Pressure Orifices

BSCW x/c		B64A010 x/c		B0012 x/c	
Upper	Lower	Upper	Lower	Upper	Lower
0.000		0.000		0.000	
0.010	0.010	0.010	0.010	0.010	0.010
0.025	0.025	0.025	0.025	0.020	0.020
0.050	0.050	0.050	0.050	0.030	0.030
0.100	0.100	0.100	0.100	0.040	
0.150		0.150		0.050	0.050
0.200	0.200	0.200	0.200	0.100	0.100
0.250		0.250		0.200	0.200
0.300	0.300	0.300	0.300	0.250	
0.350		0.350		0.300	0.300
0.400	0.400	0.400	0.400	0.350	
0.450		0.450		0.400	0.400
0.500	0.500	0.500	0.500	0.450	
0.550	0.550	0.550	0.550	0.500	0.500
0.600	0.600	0.600	0.600	0.550	
0.650	0.650	0.650	0.650	0.600	0.600
0.700	0.700	0.700	0.700	0.650	
0.750	0.750	0.750	0.750	0.700	0.700
0.800	0.800	0.800	0.800	0.750	
0.850	0.850	0.850	0.850	0.800	0.800
0.900	0.900	0.900	0.900	0.850	
0.950	0.950	0.950	0.950	0.900	0.900
1.000		1.000		0.950	0.950
				1.000	

Table 4. Locations of Pressure Orifices on the Splitter-Plate

x, in.	y, in.	z, in.
Horizontal Row		
64	0	0
48	0	0
24	0	0
20	0	0
16	0	0
0	0	0
-4	0	0
-8	0	0
-32	0	0
-48	0	0
Vertical Row 1		
0	0	16
0	0	8
0	0	4
0	0	-4
0	0	-16
Vertical Row 2		
16	0	16
16	0	8
16	0	4
16	0	-4
16	0	-16
Boundary Layer Rake		
32	0.25	16
32	0.50	16
32	0.75	16
32	1.00	16
32	1.50	16
32	2.00	16
32	2.50	16
32	3.00	16
32	4.00	16
32	5.00	16

Table 5. Design Ordinates for SC(2)-0414 and B64A010 Airfoils
(a) SC(2)-0414 Airfoil Design Coordinates

x/c	z/c upper	z/c lower	x/c	z/c upper	z/c lower
0.00000	0.00000	0.00000	0.50000	0.06840	-0.06420
0.00200	0.01080	-0.01080	0.51000	0.06800	-0.06330
0.00500	0.01660	-0.01660	0.52000	0.06760	-0.06230
0.01000	0.02250	-0.02250	0.53000	0.06720	-0.06120
0.02000	0.02990	-0.02990	0.54000	0.06670	-0.06000
0.03000	0.03500	-0.03500	0.55000	0.06620	-0.05870
0.04000	0.03890	-0.03890	0.56000	0.06560	-0.05730
0.05000	0.04210	-0.04210	0.57000	0.06500	-0.05580
0.06000	0.04480	-0.04480	0.58000	0.06430	-0.05430
0.07000	0.04710	-0.04720	0.59000	0.06360	-0.05270
0.08000	0.04910	-0.04930	0.60000	0.06280	-0.05100
0.09000	0.05100	-0.05120	0.61000	0.06200	-0.04920
0.10000	0.05270	-0.05290	0.62000	0.06110	-0.04740
0.11000	0.05420	-0.05450	0.63000	0.06020	-0.04550
0.12000	0.05560	-0.05600	0.64000	0.05930	-0.04350
0.13000	0.05690	-0.05730	0.65000	0.05830	-0.04150
0.14000	0.05810	-0.05850	0.66000	0.05730	-0.03940
0.15000	0.05920	-0.05970	0.67000	0.05620	-0.03730
0.16000	0.06020	-0.06080	0.68000	0.05510	-0.03520
0.17000	0.06120	-0.06180	0.69000	0.05400	-0.03300
0.18000	0.06210	-0.06270	0.70000	0.05280	-0.03080
0.19000	0.06290	-0.06360	0.71000	0.05160	-0.02860
0.20000	0.06370	-0.06440	0.72000	0.05030	-0.02640
0.21000	0.06440	-0.06510	0.73000	0.04900	-0.02420
0.22000	0.06510	-0.06580	0.74000	0.04770	-0.02200
0.23000	0.06570	-0.06640	0.75000	0.04640	-0.01980
0.24000	0.06630	-0.06700	0.76000	0.04500	-0.01770
0.25000	0.06680	-0.06750	0.77000	0.04360	-0.01560
0.26000	0.06730	-0.06800	0.78000	0.04220	-0.01360
0.27000	0.06770	-0.06840	0.79000	0.04070	-0.01160
0.28000	0.06810	-0.06880	0.80000	0.03920	-0.00970
0.29000	0.06850	-0.06910	0.81000	0.03770	-0.00780
0.30000	0.06880	-0.06940	0.82000	0.03620	-0.00600
0.31000	0.06910	-0.06960	0.83000	0.03460	-0.00430
0.32000	0.06930	-0.06980	0.84000	0.03300	-0.00270
0.33000	0.06950	-0.06990	0.85000	0.03140	-0.00120
0.34000	0.06970	-0.07000	0.86000	0.02980	0.00010
0.35000	0.06990	-0.07000	0.87000	0.02810	0.00130
0.36000	0.07000	-0.07000	0.88000	0.02640	0.00230
0.37000	0.07010	-0.06990	0.89000	0.02470	0.00320
0.38000	0.07020	-0.06980	0.90000	0.02290	0.00390
0.39000	0.07020	-0.06970	0.91000	0.02110	0.00440
0.40000	0.07020	-0.06950	0.92000	0.01930	0.00460
0.41000	0.07020	-0.06930	0.93000	0.01750	0.00460
0.42000	0.07010	-0.06900	0.94000	0.01560	0.00430
0.43000	0.07000	-0.06860	0.95000	0.01370	0.00380
0.44000	0.06990	-0.06820	0.96000	0.01170	0.00310
0.45000	0.06970	-0.06770	0.97000	0.00970	0.00210
0.46000	0.06950	-0.06720	0.98000	0.00760	0.00080
0.47000	0.06930	-0.06660	0.99000	0.00550	-0.00080
0.48000	0.06900	-0.06590	1.00000	0.00330	-0.00270
0.49000	0.06870	-0.06510			

Table 5. Concluded
(b) B64A010 Airfoil Design Coordinates

x/c	z/c	x/c	z/c
.000000	.000000	.490000	.047344
.001000	.003622	.500000	.046851
.002000	.005124	.510000	.046323
.005000	.008035	.520000	.045761
.010000	.011193	.530000	.045166
.020000	.015365	.540000	.044541
.030000	.018465	.550000	.043886
.040000	.021129	.560000	.043203
.050000	.023452	.570000	.042494
.060000	.025502	.580000	.041758
.070000	.027340	.590000	.040997
.080000	.029021	.600000	.040212
.090000	.030583	.610000	.039404
.100000	.032043	.620000	.038574
.110000	.033417	.630000	.037722
.120000	.034713	.640000	.036850
.130000	.035935	.650000	.035959
.140000	.037087	.660000	.035050
.150000	.038173	.670000	.034124
.160000	.039198	.680000	.033183
.170000	.040165	.690000	.032229
.180000	.041076	.700000	.031263
.190000	.041934	.710000	.030287
.200000	.042741	.720000	.029302
.210000	.043500	.730000	.028310
.220000	.044212	.740000	.027313
.230000	.044880	.750000	.026312
.240000	.045504	.760000	.025308
.250000	.046085	.770000	.024304
.260000	.046627	.780000	.023298
.270000	.047127	.790000	.022292
.280000	.047588	.800000	.021286
.290000	.048010	.810000	.020281
.300000	.048391	.820000	.019277
.310000	.048734	.830000	.018274
.320000	.049036	.840000	.017271
.330000	.049298	.850000	.016269
.340000	.049517	.860000	.015267
.350000	.049694	.870000	.014266
.360000	.049826	.880000	.013264
.370000	.049914	.890000	.012263
.380000	.049956	.900000	.011262
.390000	.049951	.910000	.010261
.400000	.049898	.920000	.009260
.410000	.049798	.930000	.008259
.420000	.049649	.940000	.007258
.430000	.049453	.950000	.006257
.440000	.049211	.960000	.005255
.450000	.048923	.970000	.004254
.460000	.048591	.980000	.003253
.470000	.048216	.990000	.002251
.480000	.047800	1.000000	.001250

Table 6. Experimental Flutter Results for BSCW in R-12 with Fixed Transition Using #35 Grit

Test Case No.	Point No.	α_m deg	M	q lb/ft^2	a ft/sec	V ft/sec	ρ slugs/ft3	R_n x10-6	μ	V_I	f_f Hz	f_f / f_θ	k	|h| in.	ϕ_h deg	|θ| deg
Classical Flutter in R-12 with Fixed Transition, #35 Grit																
7ESWFC1	492	-0.3	.435	157.4	506.5	220.4	.006482	7.03	253	.630	4.53	.863	.0861	.28	-172.5	1.20
7ESWFC2	488	-0.2	.579	162.4	508.0	294.2	.003752	5.44	437	.640	4.45	.848	.0633	.29	-174.0	1.03
7ESWFC3	485	-0.2	.689	169.3	507.9	350.0	.002764	4.77	593	.654	4.35	.829	.0521	.49	-174.7	1.42
7ESWFC4	480	-0.1	.742	168.8	506.6	375.7	.002392	4.45	685	.653	4.30	.819	.0480	.38	-175.2	1.01
7ESWFC5	465	0.0	.797	172.6	510.9	407.4	.002080	4.15	788	.660	4.14	.789	.0425	.70	-173.9	1.40
7ESWFC6	472	0.0	.803	170.7	510.0	409.3	.002038	4.09	805	.656	4.15	.790	.0424	.37	-174.8	0.73
7ESWFC7	457	1.3	.799	166.9	509.7	407.3	.002012	4.03	815	.649	4.14	.789	.0425	.35	-174.5	0.69
7ESWFC8	470	0.0	.817	178.8	511.5	417.7	.002050	4.19	800	.672	4.05	.771	.0407	.62	-173.4	1.01
7ESWFC9	466	0.0	.823	177.5	510.0	419.7	.002016	4.16	813	.669	4.13	.787	.0412	.24	-174.5	0.42
Classical Flutter in Air with Fixed Transition, #35 Grit																
7ESWFC10	341	0.0	.335	155.5	1139.	381.9	.002132	2.81	769	.626	4.55	.867	.0499	.25	-175.8	1.09
7ESWFC11	333	-0.2	.503	160.1	1132.	569.5	.000987	1.96	1660	.636	4.47	.851	.0329	.37	-176.7	1.37
7ESWFC12	329	-0.4	.619	168.2	1125.	696.9	.000693	1.71	2366	.652	4.39	.836	.0264	.57	-177.0	1.74
7ESWFC13	321	-0.1	.679	171.1	1123.	763.0	.000588	1.59	2789	.657	4.36	.830	.0239	.37	-177.0	1.08
7ESWFC14	319	-0.1	.738	177.6	1118.	825.0	.000522	1.53	3142	.669	4.27	.813	.0217	.51	-176.8	1.26
7ESWFC15	315	-0.1	.762	173.8	1116.	850.8	.000480	1.45	3413	.662	4.23	.806	.0208	.31	-177.5	0.73
Classical Flutter in Air with Free Transition																
7ESWFC16	72	-0.1	.319	140.3	1142.	364.4	.002113	2.65	776	.595	4.60	.876	.0529	.21	-175.4	1.05
7ESWFC17	57	0.0	.509	152.2	1130.	574.7	.000922	1.85	1779	.620	4.47	.851	.0326	.21	-176.3	0.86
7ESWFC18	141	-0.2	.730	172.4	1120.	817.6	.000516	1.49	3569	.622	4.23	.806	.0217	.59	-176.6	1.47
7ESWFC19	133	0.0	.769	168.9	1115.	857.6	.000459	1.41	3178	.692	4.14	.789	.0202	.44	-176.3	0.94
7ESWFC20	74	1.0	.326	145.1	1140.	372.0	.002097	2.69	782	.605	4.55	.867	.0513	.26	-175.1	1.23
7ESWFC21	60	1.0	.513	156.4	1130.	580.0	.000930	1.89	1763	.628	4.43	.844	.0320	.28	-175.8	1.12
7ESWFC22	139	1.2	.725	170.2	1121.	812.4	.000516	1.48	3180	.655	4.19	.798	.0216	.71	-175.7	1.94
7ESWFC23	137	1.2	.766	169.3	1118.	856.8	.000461	1.40	3556	.653	4.09	.779	.0200	.82	-175.4	1.92
Stall Flutter in R-12 with Fixed Transition, #35 Grit																
7ESWFS1	427	5.4	.801	124.7	507.2	406.1	.001512	3.04	1084	.561	4.87	.928	.0503	.08	-162.9	0.69
7ESWFS2	403	5.3	.799	105.5	505.6	404.0	.001293	2.60	1268	.516	4.89	.931	.0507	.05	-168.0	0.43
7ESWFS3	395	5.5	.798	93.6	503.6	402.0	.001158	2.33	1416	.486	4.97	.947	.0518	.08	-167.5	0.90

Table 7. Experimental Classical Flutter Results for B0012 in Air with Fixed Transition Using #35 Grit

Test Case No.	Point No.	α_m deg	M	q lb/ft^2	a ft/sec	V ft/sec	ρ slugs/ft3	R_n x10-6	μ	V_I	f_f Hz	f_f / f_θ	k	$\lvert h \rvert$ in.	ϕ_h deg	$\lvert \theta \rvert$ deg
7E12FC1	94	.07	0.30	131.7	1127.2	338.2	0.002303	2.736	696	0.538	4.56	0.877	0.0565	0.27	-175.5	1.63
7E12FC2	84	.07	0.39	137.2	1132.3	441.6	0.001407	2.168	1139	0.549	4.51	0.867	0.0428	0.35	-176.2	1.93
7E12FC3	79	.06	0.45	137.7	1129.5	508.3	0.001066	1.897	1503	0.550	4.47	0.860	0.0368	0.23	-176.7	1.22
7E12FC4	74	.06	0.51	141.9	1121.6	572.0	0.000867	1.755	1848	0.558	4.43	0.852	0.0324	0.32	-177.0	1.49
7E12FC5	67	.05	0.61	144.6	1108.8	676.4	0.000632	1.540	2535	0.564	4.34	0.835	0.0269	0.25	-177.3	1.01
7E12FC6	62	.05	0.67	146.5	1096.0	734.3	0.000543	1.463	2951	0.567	4.28	0.823	0.0244	0.34	-177.1	1.22
7E12FC7	48	.04	0.71	146.9	1106.6	785.7	0.000476	1.316	3366	0.568	4.25	0.817	0.0227	0.26	-177.2	0.89
7E12FC8	42	.07	0.77	144.2	1097.1	844.8	0.000404	1.251	3966	0.563	4.13	0.794	0.0205	0.36	-177.1	0.99
7E12FC9	129	.06	0.80	147.2	1109.1	887.3	0.000374	1.196	4284	0.567	4.09	0.787	0.0193	0.25	-177.4	0.60
7E12FC10	134	.07	0.82	159.9	1111.6	911.5	0.000385	1.259	4162	0.593	4.07	0.783	0.0187	0.21	-176.5	0.42

Table 8. Experimental Flutter Results for B64A010 in R-12 with Fixed Transition Using #35 Grit

Test Case No.	Point No.	α_m deg	M	q lb/ft^2	a ft/sec	V ft/sec	ρ slugs/ft3	R_n x10-6	μ	V_I	f_f Hz	f_f / f_θ	k	|h| in.	ϕ_h deg	|θ| deg
Classical Flutter																
7E64FC1	256	0.48	0.543	148.7	500.9	272.0	0.004020	5.57	405	0.619	4.462	0.856	0.069	0.3	-174.3	1.26
7E64FC2	253	0.48	0.588	149.4	500.9	294.5	0.003446	5.18	472	0.621	4.440	0.852	0.063	0.3	-173.9	1.23
7E64FC3	250	0.48	0.630	150.8	500.6	315.4	0.003033	4.89	537	0.624	4.407	0.846	0.059	0.2	-174.0	0.80
7E64FC4	246	0.48	0.674	152.8	500.6	337.4	0.002685	4.64	606	0.628	4.370	0.839	0.054	0.3	-174.3	0.98
7E64FC5	242	0.48	0.691	152.3	499.7	345.3	0.002554	4.54	637	0.627	4.365	0.838	0.053	0.2	-174.5	0.90
7E64FC6	326	0.43	0.728	158.0	503.4	366.5	0.002352	4.37	692	0.638	4.300	0.825	0.049	0.5	-174.4	1.49
7E64FC7	236	0.48	0.731	158.8	502.1	367.0	0.002359	4.42	690	0.640	4.286	0.823	0.049	0.4	-174.3	1.32
7E64FC8	230	0.48	0.742	156.1	501.6	372.2	0.002255	4.29	722	0.635	4.290	0.823	0.048	0.3	-174.7	0.93
7E64FC9	226	0.48	0.750	153.7	500.5	375.4	0.002182	4.20	746	0.630	4.296	0.825	0.048	0.2	-174.3	0.64
7E64FC10	222	0.47	0.781	159.2	500.8	391.1	0.002082	4.18	782	0.641	4.218	0.810	0.045	0.4	-174.3	1.07
7E64FC11	322	0.43	0.781	159.8	503.3	393.1	0.002069	4.13	787	0.642	4.228	0.812	0.045	0.6	-174.5	1.58
7E64FC12	218	0.40	0.799	159.8	501.3	400.5	0.001993	4.09	817	0.642	4.192	0.805	0.044	0.3	-174.3	0.77
7E64FC13	317	0.42	0.801	159.2	503.7	403.5	0.001956	4.01	832	0.641	4.200	0.806	0.044	0.3	-174.8	0.82
7E64FC14	215	0.46	0.816	159.6	500.5	408.4	0.001914	4.02	851	0.642	4.162	0.799	0.043	0.3	-174.3	0.72
7E64FC15	373	0.45	0.856	174.5	504.3	431.7	0.001873	4.10	869	0.671	4.070	0.781	0.040	0.3	-173.7	0.59
7E64FC16	311	0.42	0.861	176.8	502.8	432.9	0.001887	4.16	863	0.675	4.090	0.785	0.040	0.2	-172.2	0.42
Plunge Flutter																
7E64FP1	299	0.00	0.937	178.7	502.5	470.8	0.001613	3.88	1009	0.679	3.592	0.689	0.032	0.4	-174.3	0.91
7E64FP2	290	-0.10	0.947	172.5	502.7	476.1	0.001523	3.70	1069	0.667	3.600	0.691	0.032	0.4	-174.5	0.82

Table 9. Conditions for Static Test Cases for BSCW in R-12 with Fixed Transition, #35 Grit

Test Case No.	Point No.	M	α deg.	q psf	Wind-Off Zero Point No.
7ESWA1	608	0.582	-2.83	169.4	597
7ESWA2	609	0.583	-1.84	169.6	597
7ESWA3	610	0.583	-0.86	169.6	597
7ESWA4	611	0.581	0.10	168.8	597
7ESWA5	612	0.583	0.62	169.8	597
7ESWA6	613	0.583	1.15	169.7	597
7ESWA7	614	0.582	2.11	169.3	597
7ESWA8	615	0.583	3.14	169.7	597
7ESWA9	616	0.581	4.14	169.1	597
7ESWA10	617	0.582	4.83	169.3	597
7ESWA11	582	0.741	-2.88	170.2	581
7ESWA12	583	0.741	-1.90	170.3	581
7ESWA13	584	0.740	-0.91	170.1	581
7ESWA14	585	0.739	0.20	169.9	581
7ESWA15	586	0.739	0.65	170.0	581
7ESWA16	587	0.741	1.15	170.7	581
7ESWA17	588	0.740	2.24	170.3	581
7ESWA18	589	0.740	3.15	170.6	581
7ESWA19	590	0.741	4.16	170.9	581
7ESWA20	591	0.738	4.89	170.1	581
7ESWA21	550	0.803	-2.88	169.7	539
7ESWA22	551	0.803	-1.85	169.6	539
7ESWA23	552	0.801	-0.90	169.3	539
7ESWA24	553	0.802	0.10	169.7	539
7ESWA25	554	0.801	0.62	169.5	539
7ESWA26	555	0.802	1.10	169.8	539
7ESWA27	556	0.802	2.12	169.9	539
7ESWA28	557	0.803	3.12	170.1	539
7ESWA29	558	0.802	4.12	170.1	539
7ESWA30	559	0.802	4.83	170.2	539
7ESWA31	540	0.819	-2.90	169.7	539
7ESWA32	541	0.819	-1.87	169.8	539
7ESWA33	542	0.818	-0.89	169.7	539
7ESWA34	543	0.828	0.11	172.9	539
7ESWA35	544	0.820	0.63	170.5	539
7ESWA36	545	0.823	1.11	171.4	539
7ESWA37	546	0.823	2.11	171.6	539
7ESWA38	547	0.821	3.12	171.1	539
7ESWA39	548	0.820	4.10	170.9	539
7ESWA40	549	0.821	4.83	171.4	539
7ESWA41	513	0.882	-0.92	170.7	508
7ESWA42	510	0.877	0.00	170.8	508
7ESWA43	516	0.879	1.11	170.7	508
7ESWA44	518	0.875	3.09	170.1	508
7ESWA45	524	0.900	-0.97	178.7	508
7ESWA46	523	0.904	0.05	179.4	508
7ESWA47	522	0.900	1.07	178.3	508
7ESWA48	521	0.899	3.14	177.7	508

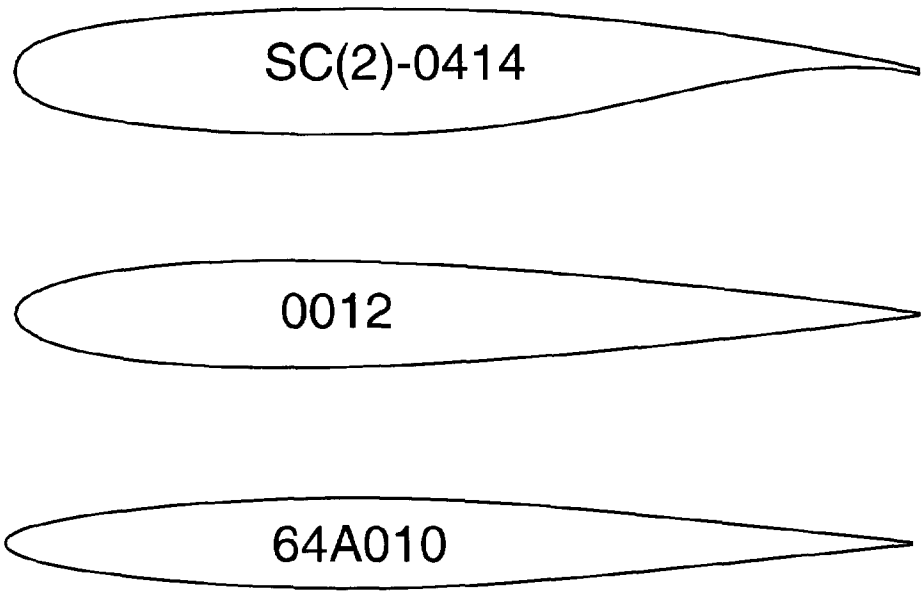

Figure 1. Airfoils used for the three Benchmark Models rectangular wings.

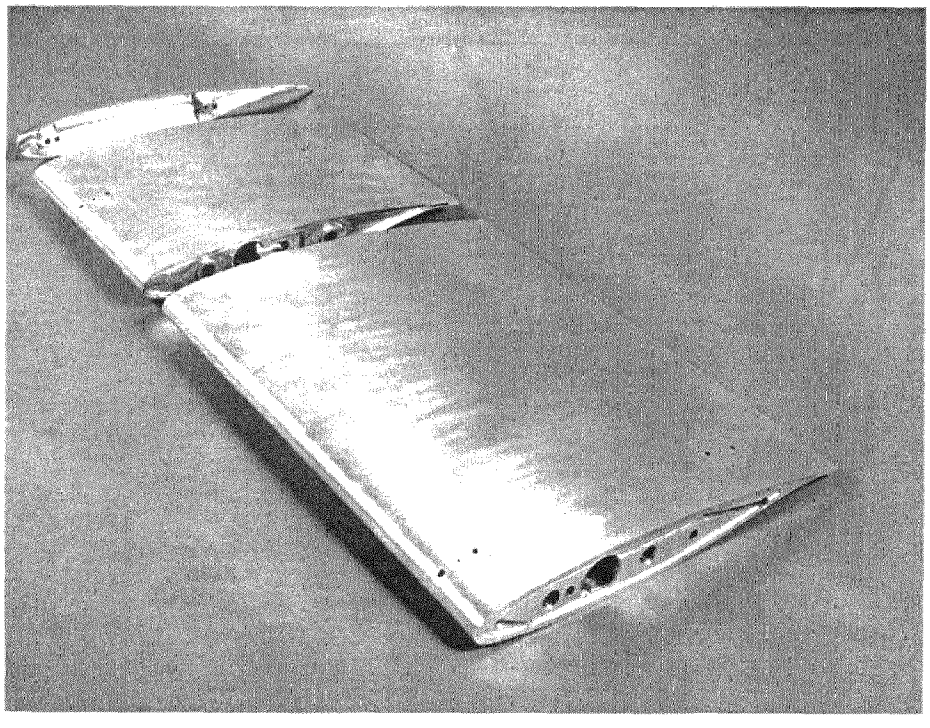

Figure 2. Photograph of Benchmark Supercritical Wing Model before assembly.

Figure 3. Photograph of Benchmark Supercritical Wing Model mounted in the wind tunnel.

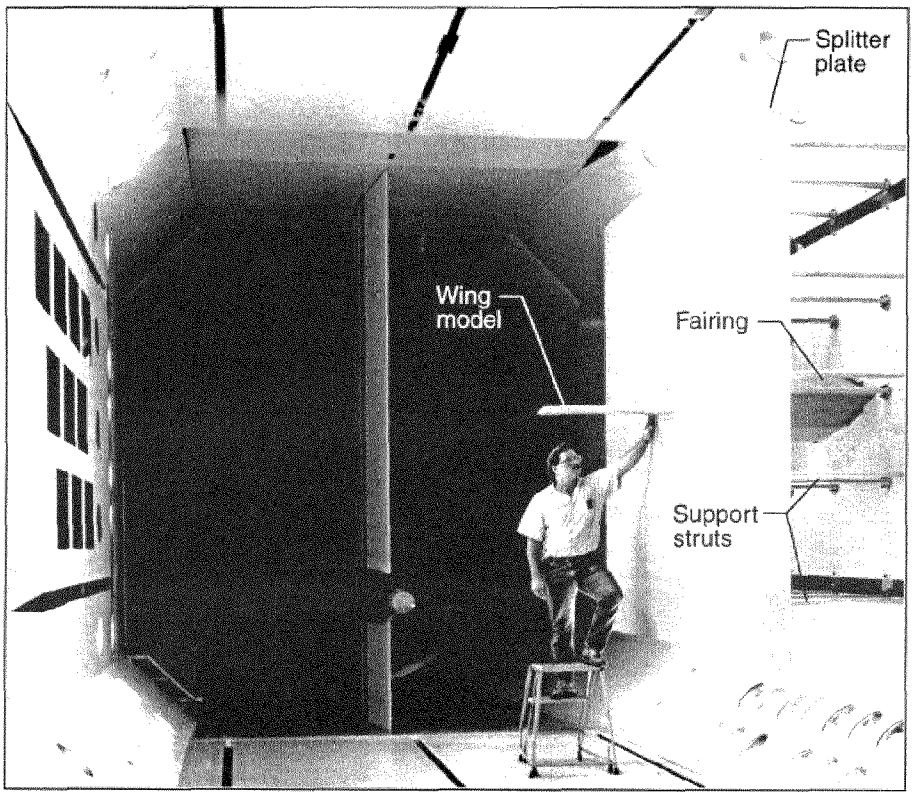

Figure 4. Photograph showing general arrangement of BSCW model and splitter plate.

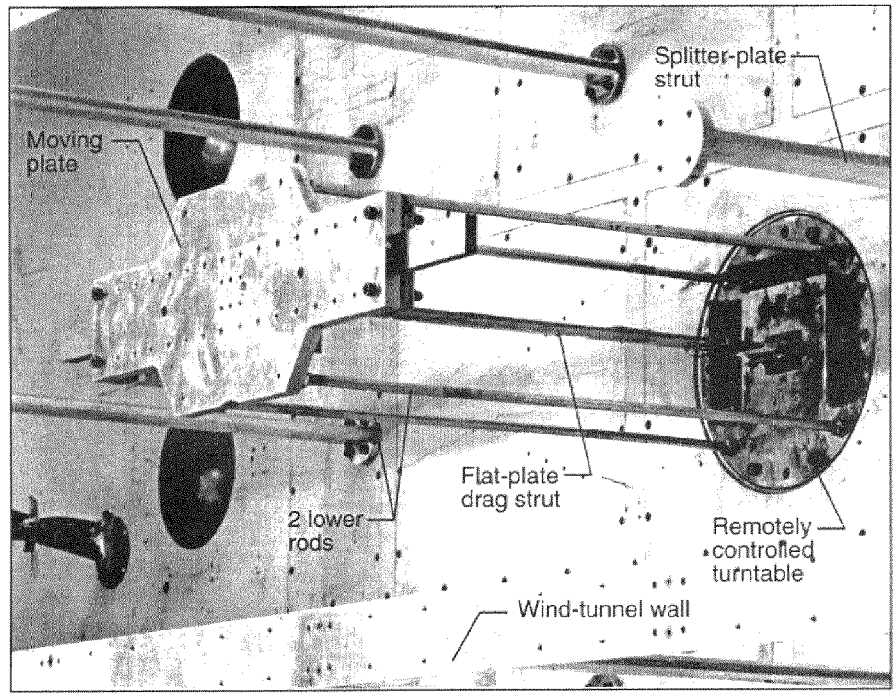

Figure 5. Photograph of Pitch and Plunge Apparatus mounted in the wind tunnel.

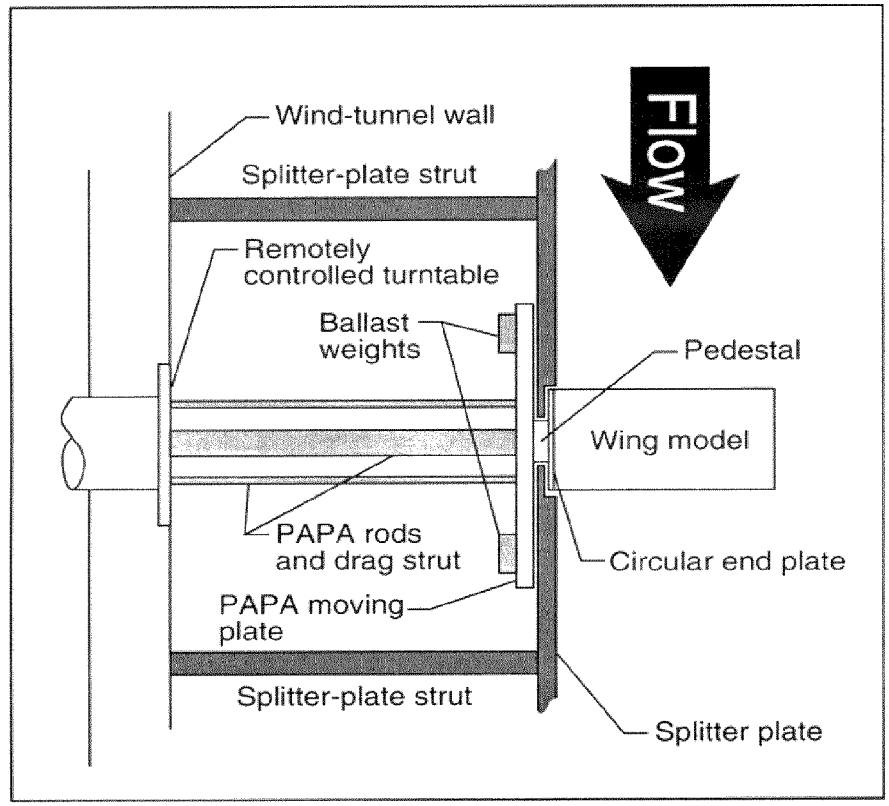

Figure 6. Sketch of model mounted on the Pitch and Plunge Apparatus.

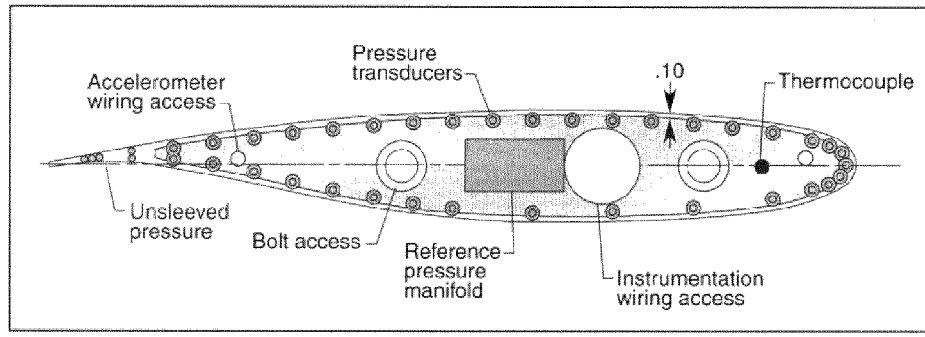

Figure 7. Pressure transducer locations on the Benchmark Supercritical Wing model.

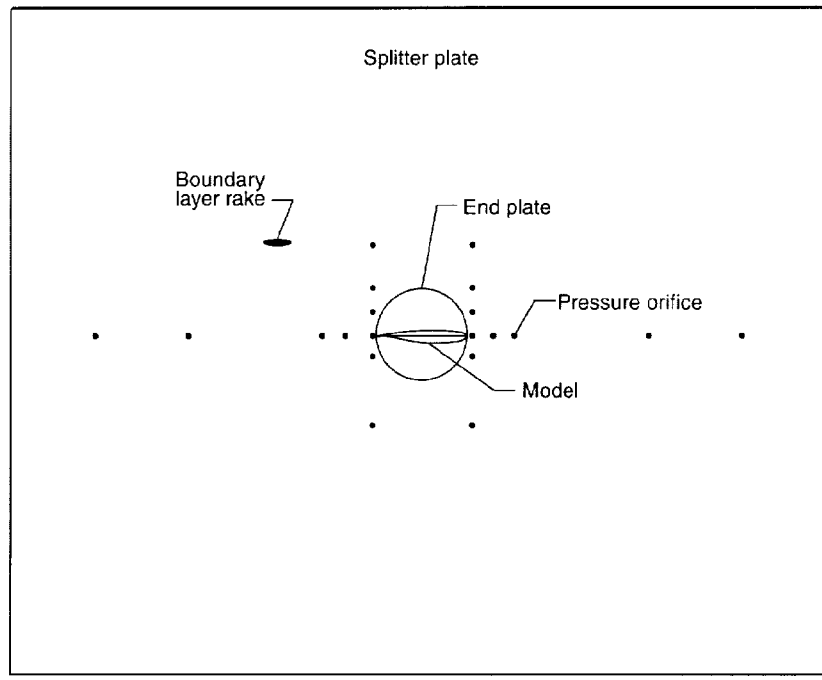

Figure 8. Sketch of pressure transducer locations on the splitter plate.

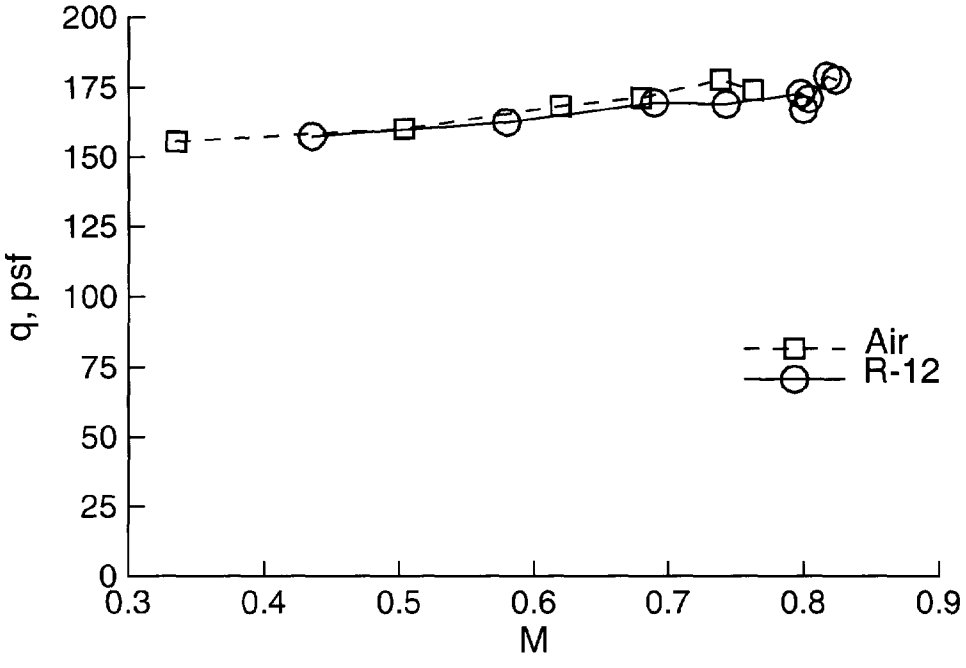

(a) Flutter dynamic pressure

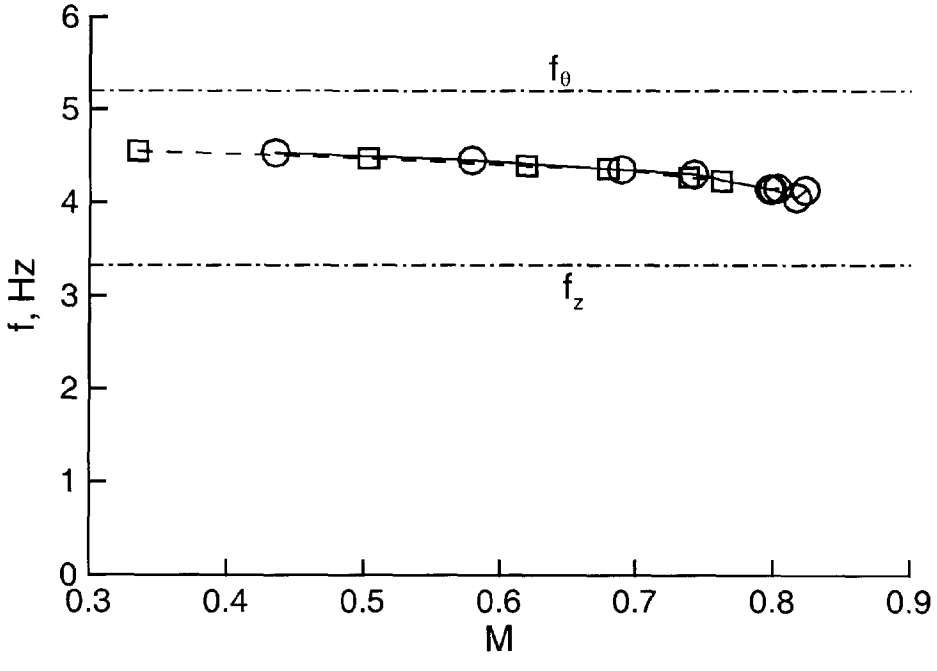

(b) Flutter frequency

Figure 9. Flutter boundaries for the BSCW in air and in R-12 (#35 grit), Test Cases 7ESWFC1-15.

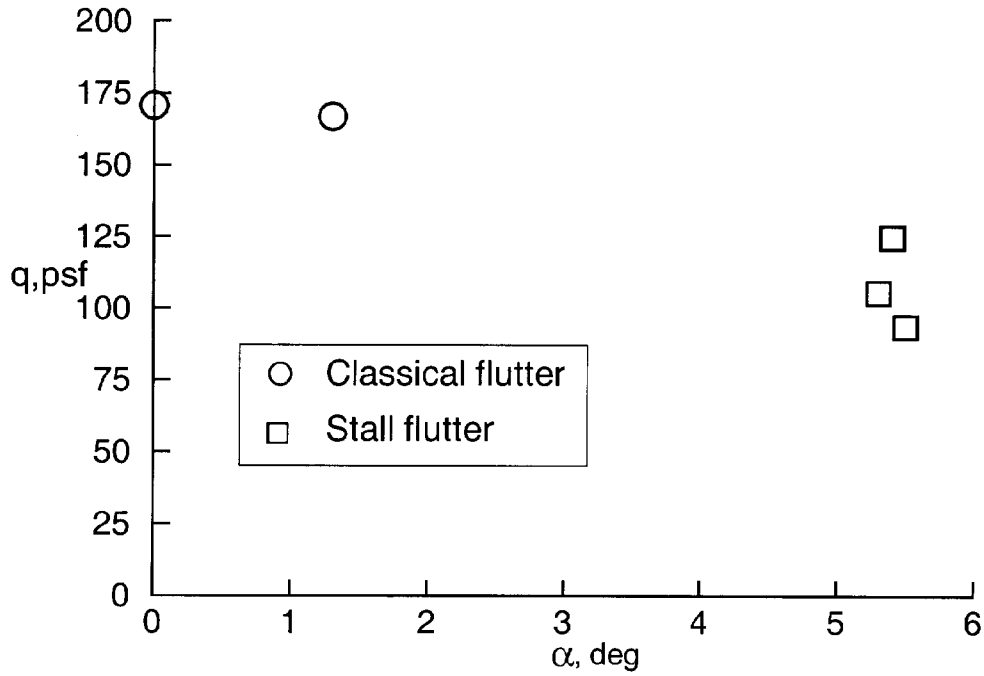

(a) Flutter dynamic pressure

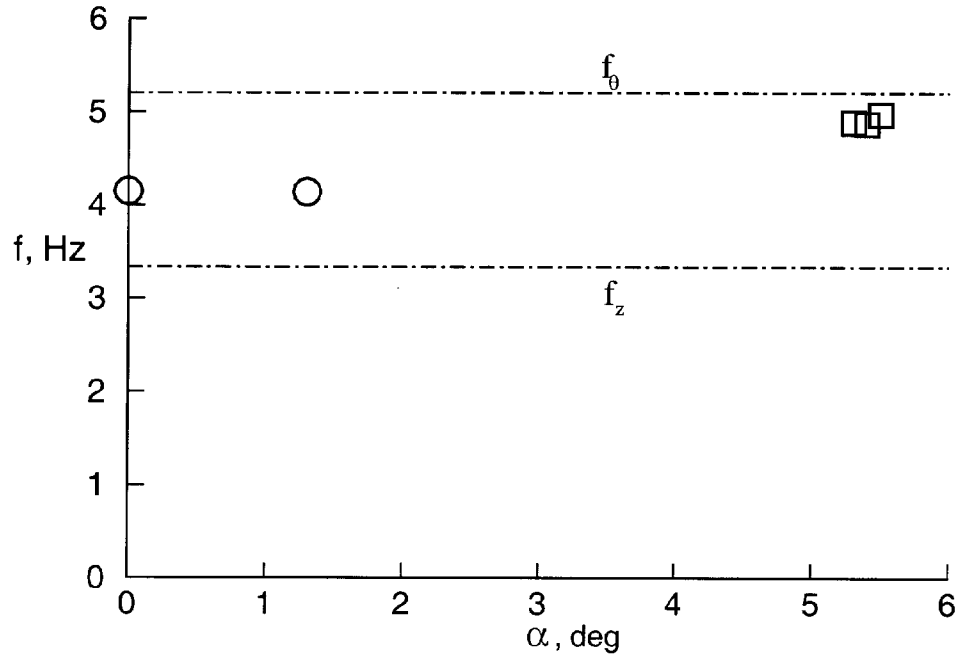

(b) Flutter frequency

Figure 10. Flutter at angle of attack for BSCW in R-12, (#35 grit), Test Cases 7ESWFS1-3, and 7ESWFC6-7, M =0.80.

Test Case	Point No	Wind-Off Zero Pt	TDT Test 470
7ESWA1	608	597	BmpBSCW/Static

Mach No	alphao,deg	q, psf	V,fps	Rn*10**-6	Prandl No	gamma
0.582	-2.83	169.4	297.0	5.72	0.748	1.136

Upper surface at ETA = 0.60

x/c	Cp Mean	Cp Min	Cp Max	CpStdDev	Chl No
0.000	0.000	0.000	0.000	0.000	1
0.010	0.546	0.499	0.585	0.013	2
0.025	0.107	0.059	0.144	0.012	3
0.050	-0.141	-0.184	-0.107	0.011	4
0.100	-0.181	-0.217	-0.150	0.009	5
0.150	-0.220	-0.252	-0.191	0.009	6
0.200	-0.249	-0.284	-0.218	0.009	7
0.250	-0.271	-0.306	-0.240	0.008	8
0.300	-0.285	-0.320	-0.252	0.009	9
0.350	-0.273	-0.304	-0.240	0.009	10
0.400	-0.289	-0.325	-0.254	0.009	11
0.450	-0.317	-0.354	-0.286	0.009	12
0.500	-0.325	-0.358	-0.293	0.009	13
0.550	-0.334	-0.366	-0.304	0.009	14
0.600	-0.302	-0.338	-0.269	0.009	15
0.650	-0.276	-0.308	-0.245	0.008	16
0.700	-0.236	-0.269	-0.204	0.009	17
0.750	-0.193	-0.227	-0.161	0.008	18
0.800	-0.166	-0.196	-0.140	0.007	19
0.850	-0.094	-0.120	-0.068	0.007	20
0.900	-0.047	-0.080	-0.021	0.007	21
0.950	0.025	-0.001	0.051	0.006	22
1.000	0.078	0.052	0.105	0.007	23

Lower surface at ETA = 0.60

x/c	Cp Mean	Cp Min	Cp Max	CpStdDev	Chl No
0.010	-0.497	-0.568	-0.442	0.019	24
0.025	-0.929	-0.995	-0.877	0.018	25
0.050	-0.915	-0.962	-0.872	0.015	26
0.100	-0.731	-0.771	-0.693	0.013	27
0.200	-0.583	-0.612	-0.555	0.009	28
0.300	-0.538	-0.571	-0.502	0.010	29
0.400	-0.496	-0.533	-0.454	0.011	30
0.500	-0.426	-0.466	-0.389	0.010	31
0.550	-0.358	-0.392	-0.325	0.009	32
0.600	-0.213	-0.247	-0.181	0.009	33
0.650	-0.087	-0.121	-0.059	0.007	34
0.700	0.048	0.019	0.074	0.008	35
0.750	0.154	0.127	0.181	0.007	36
0.800	0.232	0.210	0.257	0.006	37
0.850	0.274	0.249	0.299	0.008	38
0.900	0.314	0.289	0.337	0.007	39
0.950	0.330	0.301	0.362	0.008	40

Upper surface at ETA = 0.95

x/c	Cp Mean	Cp Min	Cp Max	CpStdDev	Chl No
0.000	1.052	1.028	1.080	0.011	69
		.			
		.			
1.000	0.000	0.000	0.000	0.000	91

Lower surface at ETA = 0.95

x/c	Cp Mean	Cp Min	Cp Max	CpStdDev	Chl No
0.010	-0.311	-0.362	-0.249	0.017	92
		.			
		.			
0.950	0.322	0.294	0.347	0.008	108

Figure 11. Example of static data file for BSCW.

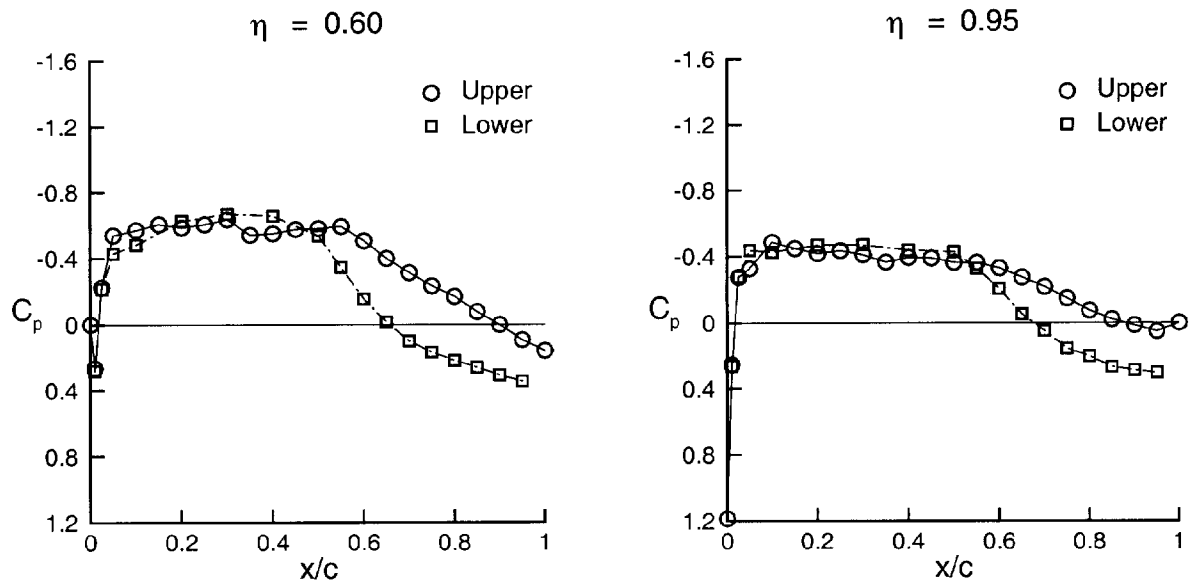

(a) Test Case 7ESWA24, α = 0.10.

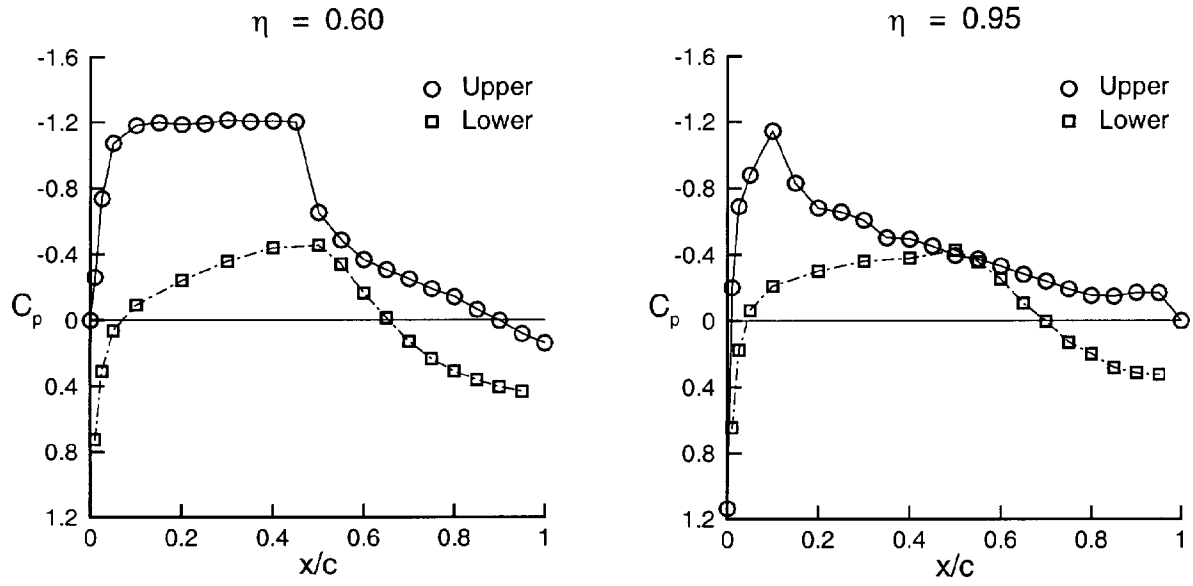

(b) Test Case 7ESWA30, α = 4.83.

Figure 12. Mean pressure coefficients for BSCW, Static Test Cases 7ESWA24and 7ESWA30, M = 0.802.

Test Case	Point No	Wind-Off Zero Pt	TDT Test 470
7ESWFC6	472	442	BmpBSCW/PAPA

Mach No	alphao,deg	q, psf	V,fps	rho,sl/ft3	Rn*10**-6	Prandl No	gamma
0.803	0.00	170.7	409.3	0.002038	4.09	0.755	1.134

FSI	ff/ft	kf	mass ratio	flt-frq,Hz	Real(h)	Imag(h)	theta,deg
0.656	0.790	0.0424	805.	4.150	-0.368	-0.034	0.73

Upper surface at ETA = 0.60

x/c	Cp Mean	Cp Min	Cp Max	CpStdDev	Real(Cp)	Imag(Cp)	Chl No
0.000	0.000	0.000	0.000	0.000	0.0000	0.0000	1
0.010	0.269	0.052	0.491	0.125	-0.1746	0.0061	2
0.025	-0.186	-0.410	0.063	0.136	-0.1889	0.0063	3
0.050	-0.412	-0.596	-0.194	0.109	-0.1516	0.0025	4
0.100	-0.665	-0.959	-0.305	0.240	-0.3233	0.0119	5
0.150	-0.613	-0.962	-0.319	0.194	-0.2477	0.0056	6
0.200	-0.557	-0.914	-0.319	0.135	-0.1511	-0.0044	7
0.250	-0.548	-0.854	-0.321	0.078	-0.0790	-0.0144	8
0.300	-0.540	-0.738	-0.328	0.078	-0.0772	-0.0152	9
0.350	-0.516	-0.749	-0.307	0.062	-0.0539	-0.0113	10
0.400	-0.532	-0.719	-0.312	0.061	-0.0468	-0.0105	11
0.450	-0.521	-0.725	-0.326	0.064	-0.0419	-0.0103	12
0.500	-0.529	-0.734	-0.315	0.065	-0.0320	-0.0097	13
0.550	-0.521	-0.748	-0.343	0.064	-0.0243	-0.0080	14
0.600	-0.464	-0.740	-0.293	0.053	-0.0124	-0.0064	15
0.650	-0.383	-0.571	-0.257	0.037	-0.0063	-0.0046	16
0.700	-0.303	-0.436	-0.198	0.031	-0.0035	-0.0035	17
0.750	-0.228	-0.344	-0.128	0.025	-0.0020	-0.0027	18
0.800	-0.142	-0.236	-0.063	0.019	-0.0011	-0.0019	19
0.850	-0.076	-0.149	-0.017	0.017	-0.0006	-0.0010	20
0.900	0.017	-0.044	0.074	0.015	-0.0011	-0.0004	21
0.950	0.111	0.065	0.167	0.013	-0.0039	-0.0004	22
1.000	0.154	0.111	0.209	0.012	-0.0086	-0.0008	23

Lower surface at ETA = 0.60

x/c	Cp Mean	Cp Min	Cp Max	CpStdDev	Real(Cp)	Imag(Cp)	Chl No
0.010	0.270	0.061	0.486	0.121	0.1683	-0.0017	24
0.025	-0.214	-0.434	0.026	0.133	0.1851	-0.0063	25
0.050	-0.311	-0.494	-0.132	0.098	0.1357	-0.0015	26
0.100	-0.671	-0.982	-0.280	0.251	0.3394	-0.0051	27
0.200	-0.638	-0.962	-0.425	0.140	0.1718	-0.0145	28
0.300	-0.624	-0.896	-0.421	0.072	0.0676	0.0163	29
0.400	-0.613	-0.857	-0.352	0.082	0.0452	0.0129	30
0.500	-0.508	-0.875	-0.299	0.075	-0.0059	0.0048	31
0.550	-0.314	-0.461	-0.195	0.035	-0.0046	0.0043	32
0.600	-0.178	-0.265	-0.084	0.023	-0.0108	0.0038	33
0.650	-0.008	-0.061	0.065	0.015	-0.0037	0.0046	34
0.700	0.098	0.040	0.160	0.015	0.0103	0.0058	35
0.750	0.164	0.092	0.226	0.021	0.0221	0.0067	36
0.800	0.206	0.140	0.274	0.025	0.0290	0.0068	37
0.850	0.251	0.173	0.322	0.028	0.0337	0.0072	38
0.900	0.284	0.203	0.351	0.029	0.0359	0.0058	39
0.950	0.329	0.245	0.400	0.029	0.0354	0.0055	40

Upper surface at ETA = 0.95

x/c	Cp Mean	Cp Min	Cp Max	CpStdDev	Real(Cp)	Imag(Cp)	Chl No
0.000	1.165	1.137	1.194	0.007	0.0026	0.0006	69
0.010	0.252	0.062	0.458	0.105	-0.1468	0.0005	70
0.900	0.004	-0.062	0.066	0.018	-0.0145	-0.0007	89
			.				
			.				
0.950	0.042	-0.040	0.108	0.024	-0.0256	-0.0009	90
1.000	0.000	0.000	0.000	0.000	0.0000	0.0000	91

Lower surface at ETA = 0.95

x/c	Cp Mean	Cp Min	Cp Max	CpStdDev	Real(Cp)	Imag(Cp)	Chl No
0.010	0.230	0.043	0.416	0.103	0.1436	-0.0016	92
0.025	-0.295	-0.498	-0.089	0.117	0.1628	-0.0035	93
			.				
			.				
0.900	0.286	0.241	0.333	0.012	0.0037	0.0019	107
0.950	0.311	0.259	0.378	0.015	-0.0070	0.0015	108

Figure 13. Example of flutter data file for BSCW.

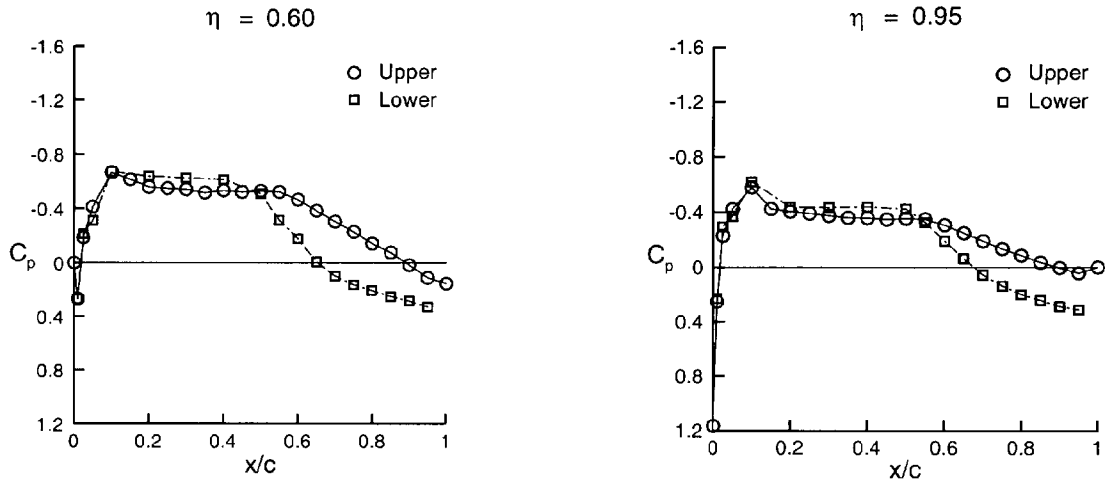

(a) Mean pressure coefficient during flutter

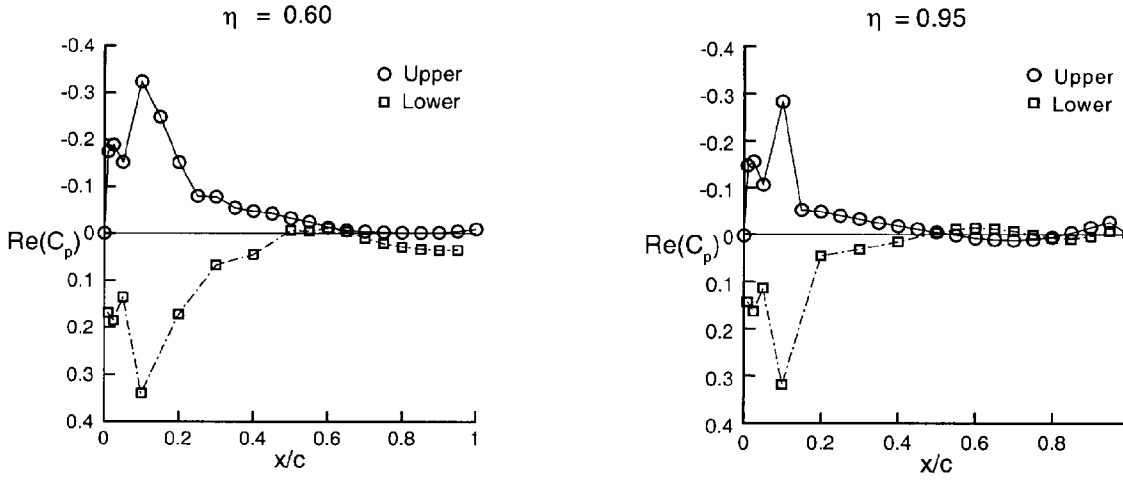

(b) Real part of pressure coefficient during flutter

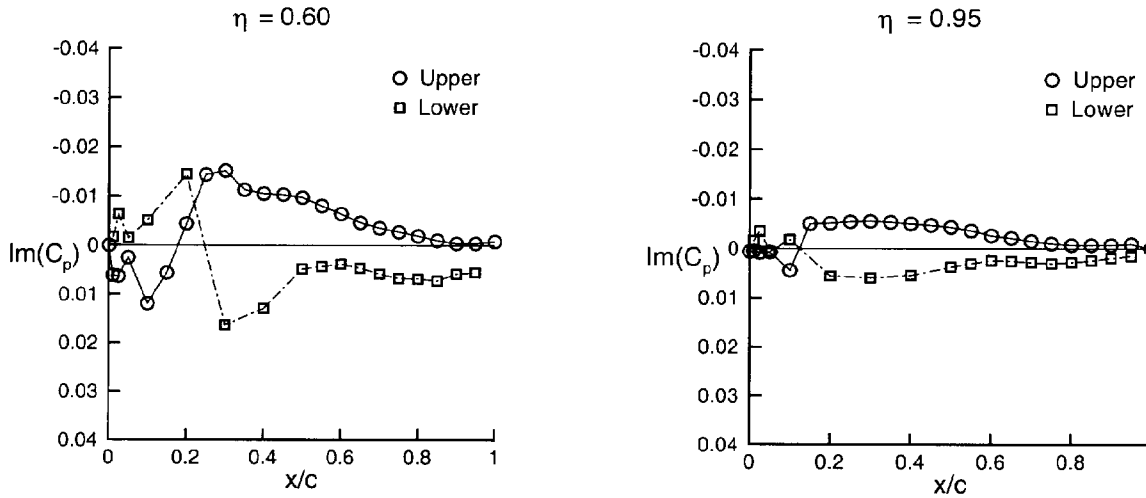

(c) Imaginary part of pressure coefficient during flutter

Figure 14. Measured pressures for BSCW during flutter, Test Case 7ESWFC6, M= 0.803, $\alpha = 0$.

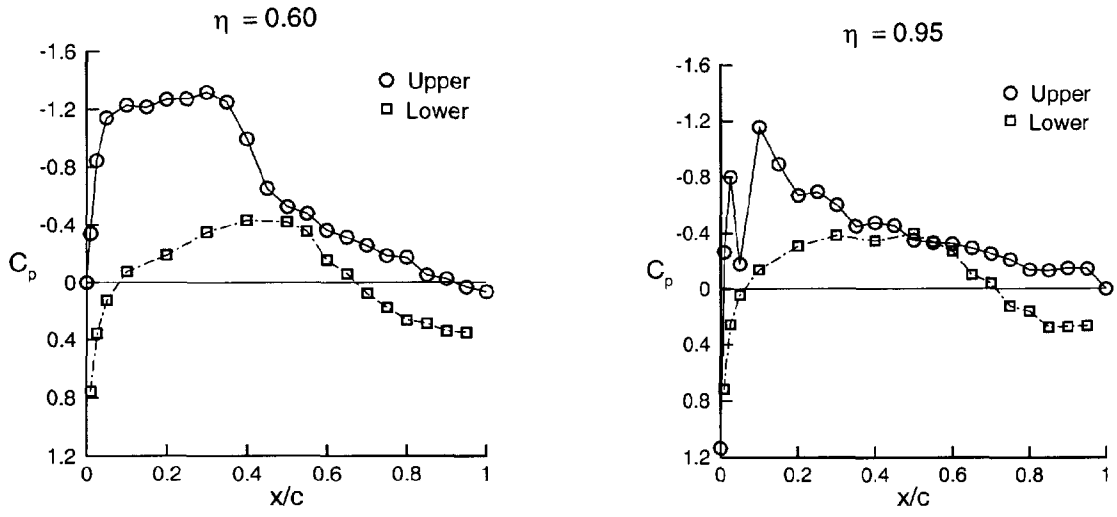

(a) Mean pressure coefficient during flutter

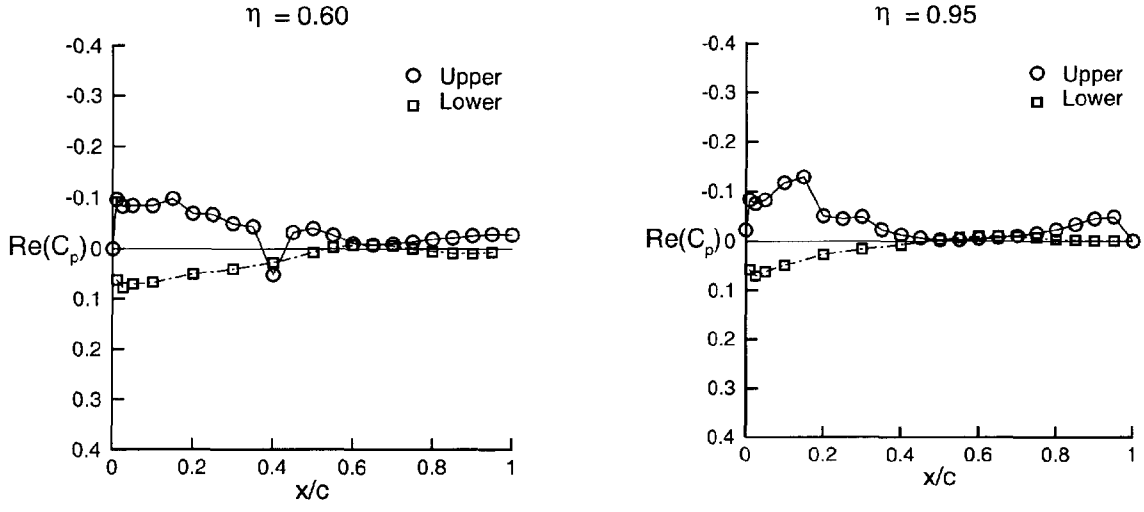

(b) Real part of pressure coefficient during flutter

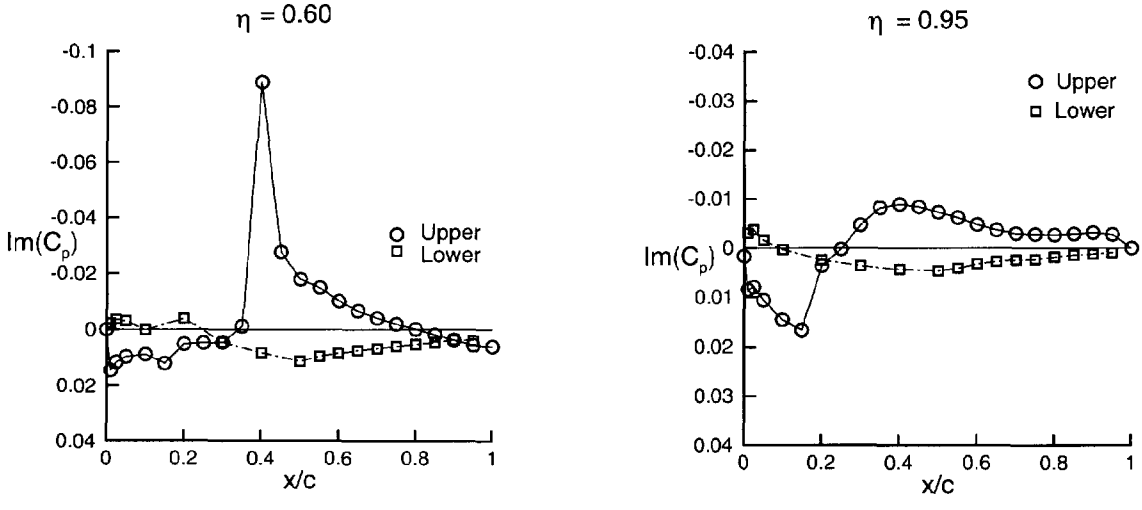

(c) Imaginary part of pressure coefficient during flutter

Figure 15. Measured pressures for BSCW during flutter, Test Case 7ESWFS3, M= 0.798, α = 5.5 degrees.